Water Science and Engineering 2016, 9(1): 52−57

HOSTED BY

ELSEVIER

CrossMark

Available online at www.sciencedirect.com

Water Science and Engineering

journal homepage: http://www.waterjournal.cn

Optimization of multi-model ensemble forecasting of typhoon waves

Shun-qi Pan [a,*], Yang-ming Fan [b], Jia-ming Chen [b], Chia-chuen Kao [c]

[a] *Hydro-environmental Research Centre, School of Engineering, Cardiff University, Cardiff CF24 3AA, UK*
[b] *Coastal Ocean Monitoring Center, National Cheng Kung University, Tainan 701, China*
[c] *Department of Hydraulic and Ocean Engineering, National Cheng Kung University, Tainan 701, China*

Received 1 July 2015; accepted 30 November 2015
Available online 13 February 2016

Abstract

Accurately forecasting ocean waves during typhoon events is extremely important in aiding the mitigation and minimization of their potential damage to the coastal infrastructure, and the protection of coastal communities. However, due to the complex hydrological and meteorological interaction and uncertainties arising from different modeling systems, quantifying the uncertainties and improving the forecasting accuracy of modeled typhoon-induced waves remain challenging. This paper presents a practical approach to optimizing model-ensemble wave heights in an attempt to improve the accuracy of real-time typhoon wave forecasting. A locally weighted learning algorithm is used to obtain the weights for the wave heights computed by the WAVEWATCH III wave model driven by winds from four different weather models (model-ensembles). The optimized weights are subsequently used to calculate the resulting wave heights from the model-ensembles. The results show that the optimization is capable of capturing the different behavioral effects of the different weather models on wave generation. Comparison with the measurements at the selected wave buoy locations shows that the optimized weights, obtained through a training process, can significantly improve the accuracy of the forecasted wave heights over the standard mean values, particularly for typhoon-induced peak waves. The results also indicate that the algorithm is easy to implement and practical for real-time wave forecasting.

Keywords: Wave modeling; Optimization; Forecasting; Typhoon waves; WAVEWATCH III; Locally weighted learning algorithm

1. Introduction

Prediction and understanding of ocean waves are extremely important for ocean-dependent industries, such as shipping and fisheries, as well as for coastal protection and coastal zone management. In particular, the highly energetic waves induced by typhoon events can cause enormous damage to property, infrastructure, and human lives (Doong et al., 2012; Liu et al., 2008). The catastrophic consequences of typhoon-related events have often been seen and reported in Taiwan in recent years. Although it is almost impossible to completely avoid the damage caused by typhoons, more accurate prediction and forecasting of typhoon-induced waves play an important role in mitigating and minimizing the impacts from the typhoons. However, the hydrological and meteorological interactions are complex, and the uncertainties arising from both weather and hydrodynamic modeling systems due to the forcing conditions, modeling techniques, and physical parameters can make wave prediction and forecasting rather difficult and challenging. In recent years, ensemble approaches have been widely used to improve quantification of the uncertainties arising from the modeling systems and physical parameters. In wave modeling, ensemble approaches can be generally classified into two types: parameter ensemble approaches and model ensemble approaches. In both types, a

This work was supported by the European Commission within FP7-THEME 6 (Grant No. 244104), the Natural Environment Research Council (NERC) of the UK (Grant No. NE/J005541/1), and the Ministry of Science and Technology (MOST) of Taiwan (Grant No. MOST 104-2221-E-006-183).

* Corresponding author.
E-mail address: PanS2@cardiff.ac.uk (Shun-qi Pan).
Peer review under responsibility of Hohai University.

http://dx.doi.org/10.1016/j.wse.2016.02.001

particular wave model is selected to transform the atmospheric forcing conditions into wave fields, but the atmospheric forcing conditions can be generated in different ways. The parameter ensemble approach generates wave ensembles through the wave model, which is driven by the ensembles of forcing conditions (usually winds and atmospheric pressure) from a weather model using equally perturbed physical parameters. For example, in the works reported by Chen et al. (2010) and Zou et al. (2013), the tide-wave model POLCOMS/ProWAM (Osuna et al., 2004) was used to produce the ensemble results of waves, tides, and storm surges from 50 ensembles of wind field and atmospheric pressure as the surface forcing. Then, statistical analysis was carried out to quantify the uncertainties arising from the model results of both hydrodynamics and morphodynamics. The model ensemble approach, in contrast, uses the ensembles of surface forcing conditions generated from different weather models, each of which is calibrated to its optimal operational conditions for a particular region or globally to drive the wave model to produce the wave ensembles for statistical analysis. In the work of Fan et al. (2013), the WAVEWATCH III model was used to transform the wind fields obtained from four weather models, namely the National Centers for Environmental Prediction (NCEP) Aviation model (AVN), Japan Meteorological Agency model (JMA), non-hydrostatic forecast system (NFS), and weather research and forecasting model (WRF), developed by different research institutions, to model ocean waves in the coastal waters of Taiwan for real-time wave forecasting. Their results showed that the mean wave heights of the waves generated by four wind fields in general agreed with the field observations from the wave buoys deployed off the Taiwan coasts. However, it was clear that, during typhoon events, the peak wave heights were generally underestimated by the standard equally weighted averaging method. As the peak wave height during the typhoon events can be one of the most important parameters in the decision- and policy-making processes since it represents the worst-case scenario, it is desirable to improve the methodology currently used to generate more accurate peak wave heights during the typhoon events. To this end, in this paper, a locally weighted learning algorithm is proposed to optimize the weights and used to calculate the resulting wave heights from each model-ensemble, so that the behavior of the wave model in response to each wind field can be better captured and understood, leading to improved typhoon wave forecasting. This study used the computed wave heights presented in Fan et al. (2013) for three typhoon events that occurred in 2011 and 2012 to illustrate the proposed methodology.

2. Wave model and computational domains

As stated in Fan et al. (2013), the WAVEWATCH III model was selected to predict waves from the surface wind forcing. For the sake of clarity, the wave model and its computational domains are briefly described here. The WAVEWATCH III wave model is a third-generation wave model developed at the National Oceanic and Atmospheric Administration/National Centers for Environmental Prediction (NOAA/NCEP) (Tolman, 1997, 1999, 2009) in the spirit of the WAM wave model (WAMDIG, 1988; Komen et al., 1994), which has been widely used to simulate wave fields using the wind data from various weather models.

In the work of Fan et al. (2013), a nested computational framework, as shown in Fig. 1, was used. The waves computed from the left-side coarse-grid domain were used to provide the boundary conditions for the right-side fine-grid domain. The resolutions of the coarse and fine grids were 0.5° (about 55 km) and 0.25° (about 27.5 km), respectively. The modeling system was driven by the wind fields from four weather models, namely, AVN, JMA, NFS, and WRF. The modeling system was applied to three typhoon events, Typhoon Jelawat, which occurred in 2012, and Typhoons Meari and Nanmadol, which occurred in 2011, as part of their operational forecasting. With four wind fields used as the surface forcing, the model generated four ensembles for waves. The wave heights of four wave ensembles were averaged using the standard arithmetical averaging method (i.e., equally weighted, 1/4). Their results, in general, showed agreement between the averaged wave heights and the measurements at a number of selected locations. However, it was clear that the averaged peak wave heights during those typhoon events were underestimated. Those peak waves, which in fact have the most

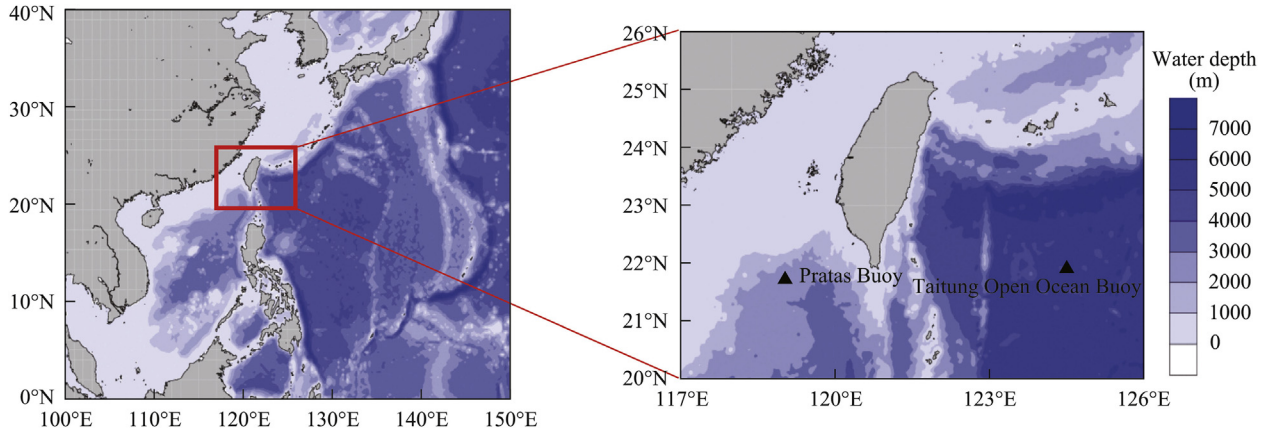

Fig. 1. Nested computational domains for WAVEWATCH III model and locations of wave buoys.

significant impacts on the coastal areas and can cause the severest damage, ought to be predicted and forecasted more accurately, so that such damage can be effectively mitigated and minimized. Close examination of the predicted wave heights showed that the wave model responded differently to different wind fields. The equally weighted averaging method might be inappropriate for calculating the mean wave heights and also incapable of representing the peak waves. Therefore, in this paper, an optimization method is proposed to generate a set of optimized weights, which can be used to improve the representation of the ensemble wave heights, especially for typhoon peak waves.

3. Optimization method

In this study, optimization was based on the concept of locally weighted learning (Atkeson et al., 1997), which is briefly described below:

Assuming that we have a set of wave heights (ensembles) generated by the wave model from different wind fields: H_i (i=1, 2,⋯, N, where N is the number of ensembles), the averaged wave height $\overline{H}$ can be calculated with the weighted averaging method:

$$\overline{H} = \sum_{i=1}^{N} w_i H_i \tag{1}$$

where w_i is the weight of the ith ensemble. When w_i=1/N, Eq. (1) represents the standard equally weighted averaging. In the optimization, w_i can be determined using the locally weighted learning algorithm, in an attempt to better represent the resulting wave heights with the aid of field measurements. When a set of measured wave heights is available at any particular location, a cost function can be established:

$$J = \frac{1}{2}\sum_{j=1}^{M}\left(\overline{H}_j - \widehat{H}_j\right)^2 \tag{2}$$

where J is the cost function, $\overline{H}_j$ is the averaged wave heights at the jth location calculated with Eq. (1), $\widehat{H}_j$ is the measured wave heights at the jth location, and M is the number of data points available. Using the least mean squares (LMS) algorithm, the gradient of the cost function J with respect to each weight can be estimated as follows:

$$\frac{\partial J}{\partial w_i} = H_i \sum_{j=1}^{M}\left(\overline{H}_j - \widehat{H}_j\right) \tag{3}$$

The parameter w_i can be calculated with the gradient descent algorithm from Eqs. (1) and (3). Writing the algorithm in matrix format for brevity yields the following equation:

$$\boldsymbol{w} = (\boldsymbol{H}^{\mathrm{T}}\boldsymbol{H})^{-1}\boldsymbol{H}^{\mathrm{T}}\widehat{\boldsymbol{H}} \tag{4}$$

where $\boldsymbol{w}$ is the N-dimensional column matrix of weights, $\boldsymbol{H}$ is the $M \times N$ matrix of the computed wave heights, and $\widehat{\boldsymbol{H}}$ is the M-dimensional column matrix of measured wave heights.

4. Training and validation

In order to obtain the weights expressed in Eq. (4), training is required. In this study, training was carried out using the model results and measurements for Typhoon Jelawat at two locations, the Taitung Open Ocean Buoy and Pratas Buoy as shown in Fig. 1. The former is located in a deep-water area (with a depth greater than 6000 m) and the latter is close to the shore. At both locations, the wave buoys deployed for the wave measurements are equipped with a tri-axial accelerometer, so that surface movements can be recorded for the estimation of a directional wave spectrum. The accuracy of the tri-axial accelerometer is 0.3924 m/s^2. As shown by Lin et al. (2015), the correlation coefficient of the significant wave heights measured by the accelerometer and the real time kinematics (RTK) GPS wave sensor was as high as 0.99, indicating a high level of accuracy for the wave measurements from the buoys.

As Typhoon Jelawat is the strongest of all three, it was expected that the weights obtained from the training could cover the widest wave height range possible in this study, and would be valid for applications to other typhoons. It should be noted that the optimized weights are location-specific. Therefore, it is necessary to carry out training at each location of interest in practice. In this study, 128 valid hourly data points out of 148 hourly measurements from 00:00 on September 24, 2012 to 00:00 on September 30, 2012 (six days) were used. Fig. 2(a) shows the computed wave heights generated by four wind fields of different weather models (denoted as H_{AVN}, H_{JMA}, H_{NFS}, and H_{WRF}, respectively) and the standard mean wave heights (denoted as H_{mean}), together with the field measurements (denoted as H_{obs}) at the Taitung Open Ocean Buoy location. As shown in the figure, a peak typhoon wave height up to 19 m was observed on September 27, 2012. In Fig. 2(a) it

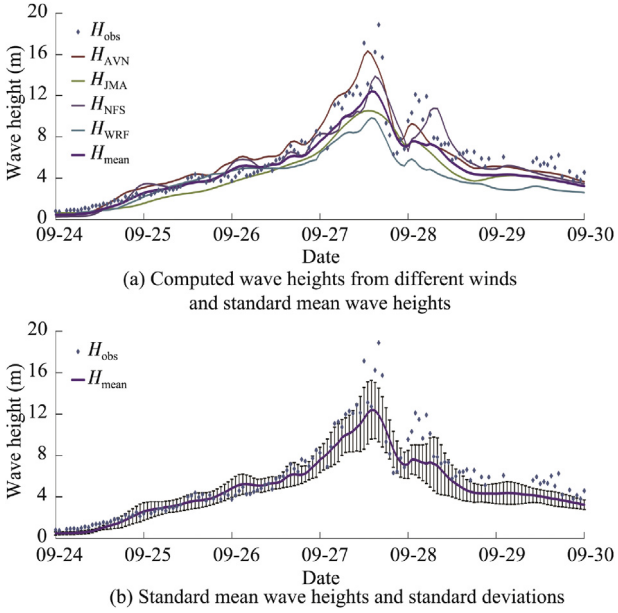

(a) Computed wave heights from different winds and standard mean wave heights

(b) Standard mean wave heights and standard deviations

Fig. 2. Comparison of computed wave heights from different winds and standard mean wave heights with observations at Taitung Open Ocean Buoy location during Typhoon Jelawat in 2012.

can also be seen that, despite the wave heights generated by the AVN winds in general agree with the observations, the computed wave height at the typhoon peak is considerably under-predicted. For the computed wave heights forced by other wind fields, the results are less satisfactory at the typhoon peak, with the worst performance from the WRF wind fields. The mean wave heights calculated with the standard averaging method from four ensembles also show a significant under-prediction at the typhoon peak, and only for less energetic waves (with wave heights less than 8 m) is the agreement seen reasonable. Fig. 2(b) shows the mean wave heights with the standard deviations as the upper/lower limits (shown as error bars). It is clear that, even when the standard deviations are considered to compensate for the mean wave heights, the wave heights at the typhoon peak are still under-predicted by more than 5 m. As indicated by the results shown in Fig. 2, there are considerable discrepancies in the wave heights generated by different wind fields, and some performed better than others. With the predicted wave heights shown, deciding which wave heights should be used for forecasting could be difficult and arbitrary. Therefore, simply averaging the wave heights from all ensembles can be insufficient to yield the desirable results, as indicated in this example.

In order to improve the accuracy of the averaged wave heights from four ensembles of the predicted waves, the locally weighted learning approach, as described in the previous section, Eq. (4), was applied to the computed and observed wave heights as a training exercise to yield a set of optimized weights. The training used all computed wave heights from four wind fields, including those generated by WRF winds, which had little capability of generating the typhoon waves as shown in Fig. 2(a), without discriminating toward any particular set of the computed wave heights, as well as the corresponding field measurements made available to this study. Table 1 lists the optimized weights from the training at both the Taitung Open Ocean Buoy and Pratas Buoy locations. At the Taitung Open Ocean Buoy location, the weight for AVN winds is clearly the highest and that for WRF winds is the lowest (negative). These values reflect the performance of the corresponding winds in generating waves, as shown in Fig. 2. At the Pratas Buoy location, however, the weights for AVN, JMA, and NFS winds have similar values, with the weight for JMA winds being slightly more favorable (having the highest value). This indicates that all three winds are generating wave heights to a reasonable degree, which is also confirmed by the measurements (not shown here). The wave heights generated by the WRF winds still remain the worst at this location in comparison with the measurements. However, as pointed out by Hunt et al. (1995), the ill-conditioned nature in the design of the matrix used in the linear locally weighted learning approach can lead to optimal weights consisting of balanced large positive and negative weights that are essential to minimizing the output error in the training set.

Table 1
Optimized weights obtained from training at Taitung Open Ocean Buoy and Pratas Buoy locations.

Location	Optimized weight			
	AVN	JMA	NFS	WRF
Taitung Open Ocean Buoy	0.9549	0.2751	0.2667	−0.6453
Pratas Buoy	0.3855	0.4937	0.3081	−0.1307

In order to validate the proposed approach, the optimized weights listed in Table 1 were then used to calculate the optimized average wave height from four ensemble wave heights, which were the same data sets used in training. Fig. 3 shows the resulting wave heights averaged using the optimized weights (H_{opt}, referred to as the optimized average wave heights hereafter), together with the standard mean wave heights (H_{mean}) and the field measurements (H_{obs}). It is clear that the optimized average wave heights agree significantly better with the measurements at the typhoon peak than the standard mean wave heights.

Fig. 4 shows scatter plots of the observed wave heights against the standard mean wave heights and optimized average wave heights at the Taitung Open Ocean Buoy and Pratas Buoy locations. The results clearly show a general improvement with the optimized average wave heights, in particular for large waves, as circled in Fig. 4(a), and for waves with heights less than 7 m. However, for waves with heights around 10 m, the optimized average wave heights are found to be larger than the measurements. Fig. 4(b) compares the optimized average wave heights with the standard mean wave heights and the observations at the Pratas Buoy location. The optimized wave heights are found to agree better with the measurements. Overall, due to the large wave heights at the Taitung Ocean Buoy location, the improvement of the optimized wave heights appears more significant in comparison with that at the Pratas Buoy location, where the water depth and wave heights are relatively smaller.

5. Applications

Following the training and validation, the weights listed in Table 1 can be applied to other typhoon events. For illustration purposes, two typhoon events, Meari and Nanmadol, which occurred in June and August 2011, respectively, were used in this study. Fig. 5 compares the optimized average wave heights with the observed wave heights at the Taitung Ocean Buoy location for both typhoons. For Typhoon Meari, shown in Fig. 5(a), the optimized average wave heights at the typhoon peak (with values greater than 6 m) agree significantly better with the measurements than the standard mean wave heights. However, for Typhoon Nanmadol, shown in Fig. 5(b), the optimized average

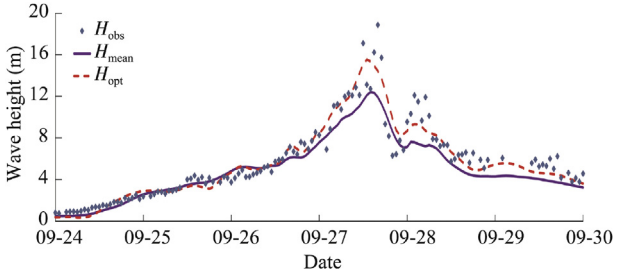

Fig. 3. Comparison of standard mean wave heights and optimized average wave heights with observations at Taitung Open Ocean Buoy location during Typhoon Jelawat in 2012.

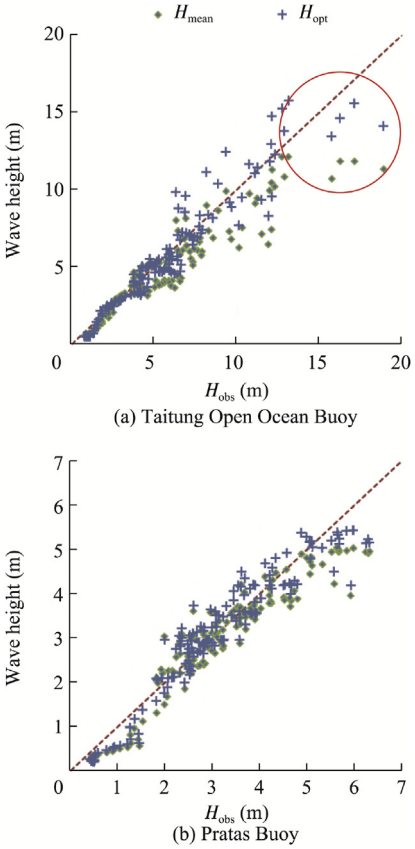

Fig. 4. Scatter plots of standard mean wave heights and optimized average wave heights versus observed wave heights at Taitung Open Ocean Buoy and Pratas Buoy locations.

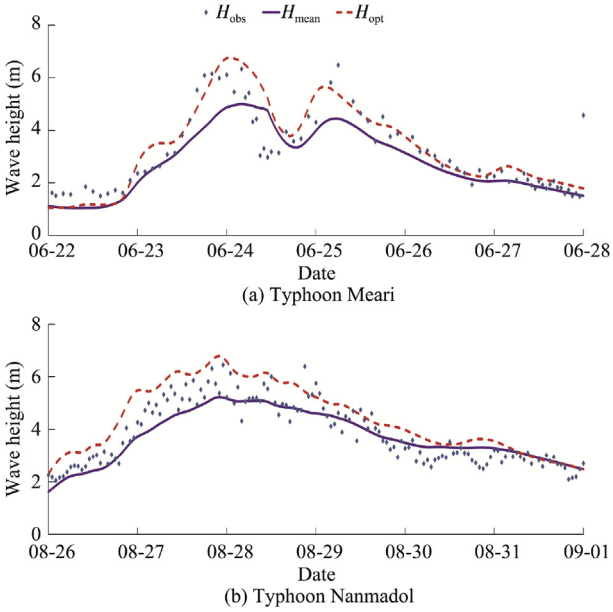

Fig. 5. Comparison of optimized average wave heights and standard mean wave heights with observations at Taitung Open Ocean Buoy location for Typhoons Meari and Nanmadol in 2011.

wave heights are greater than the measurements, while the standard mean wave heights are slightly smaller than the measurements, but both are within a close range.

Similar to Fig. 4, Fig. 6 is a scatter plot of the optimized average wave heights and the standard mean wave heights against the measurements at the Taitung Open Ocean Buoy location for both Typhoons Meari and Nanmadol. Fig. 6(a) confirms an improved agreement between the optimized average wave heights and the measured wave heights for Typhoon Meari, particularly for the wave heights greater than 6 m. The wave heights are overestimated for wave heights ranging between 3 m and 6 m. For Typhoon Nanmadol, as shown in Fig. 6(b), the optimized average wave heights are in general greater than the measurements, with an improvement for wave heights greater than 6 m.

Fig. 7 shows a similar comparison of the optimized average wave heights with the standard mean wave heights and the observations as those shown in Fig. 5 for Typhoons Meari and Namadol at the Pratas Buoy location. The results at this location indicate a general overestimation of the wave heights for both typhoon events. From Fig. 7(a), it can be seen that, for Typhoon Meari at the Pratas Buoy location, the measured wave heights are relatively small, mostly less than 3 m, but the weights obtained from the training are based on Typhoon Jelawat, with predominately large wave heights, as shown in Fig. 4(b). The discrepancies may be attributed to the fact that

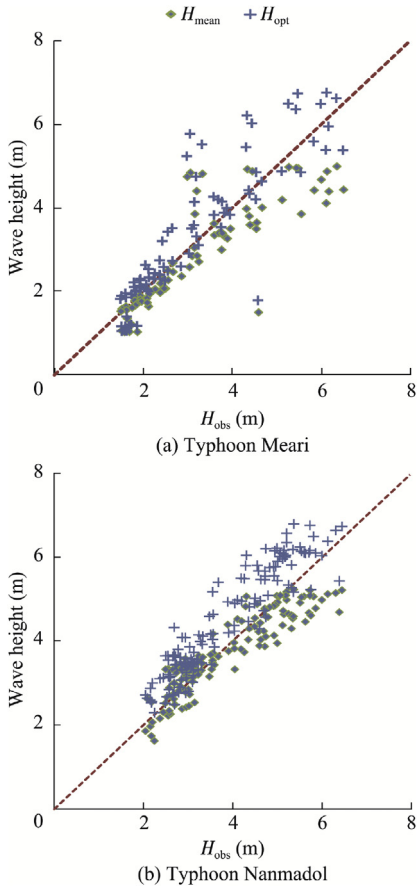

Fig. 6. Scatter plots of standard mean wave heights and optimized average wave heights versus observed wave heights at Taitung Open Ocean Buoy location for Typhoons Meari and Nanmadol.

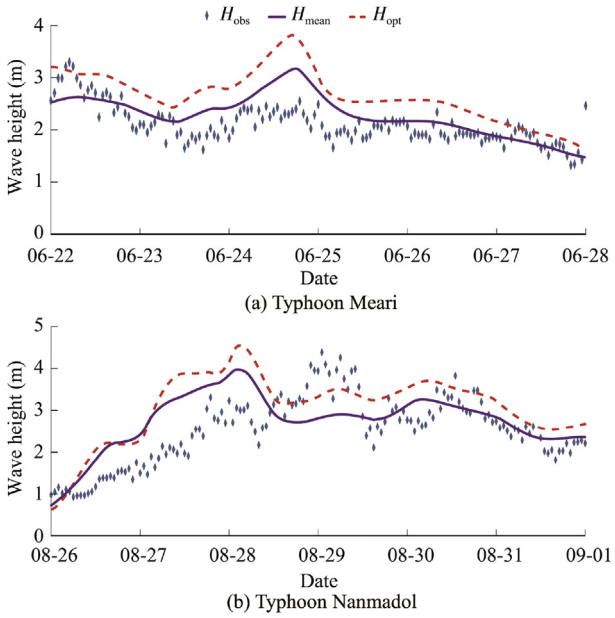

Fig. 7. Comparison of optimized average wave heights and standard mean wave heights with observations at Pratas Buoy location for Typhoons Meari and Nanmadol in 2011.

more energetic waves are used in training of the weights as previously described, resulting in the weights being biased and wave heights being over-predicted in this case. However, for the non-typhoon events when wave heights are small, the impact of these discrepancies can be regarded as insignificant.

In summary, the results presented in this paper clearly demonstrate that the locally weighted learning algorithm is capable of optimizing the model ensemble results and providing improved wave forecasting results in the coastal waters of Taiwan. In principle, the algorithm is efficient and easy to implement at particular locations, and the weights can be updated progressively for real-time wave forecasting. The inaccuracy shown in Fig. 7 also suggests the need of using a larger data set over a longer period to further improve the accuracy of the optimization.

6. Conclusions

An optimization has been applied to the model ensemble wave heights obtained from the WAVEWATCH III model, driven by wind fields of four weather models. The locally weighted learning algorithm was implemented to calculate the weights associated with each model ensemble result from a training process using the data measured during Typhoon Jelawat, which occurred in 2012, at both the Taitung Open Ocean Buoy and Pratas Buoy locations. The weights obtained from the training were then used to yield the optimized average wave heights, which were compared with the standard mean wave heights and measurements during two typhoon events in 2011, Typhoons Nanmadol and Meari. The results show a significant improvement of the optimized average wave heights over the commonly used standard mean wave heights, particularly for the typhoon-induced peak waves. It is also clear that the proposed optimization algorithm is practically well suited for and can be easily applied to the real-time wave forecasting.

However, it should be borne in mind that the results presented in this paper are based on a training over a short period, approximately six days, with only one typhoon event (Typhoon Jelawat), which is insufficient for the less energetic waves. It is expected that the results can be further improved if the training is carried out using a longer time series of model results and measurements, which will allow for the variation of weights with different ranges of wave heights to be included and fully examined, and more advanced optimization algorithms to be explored.

Acknowledgements

The authors would like to thank the Central Weather Bureau of Taiwan for providing wind and observed wave data.

References

Atkeson, C.G., Moore, A.W., Schaal, S., 1997. Locally weighted learning. Artif. Intell. Rev. 11, 11−73.

Chen, Y.P., Pan, S.Q., Hewston, R., Cluckie, I., Wolf, J., 2010. Ensemble modelling of tides, surge and waves. In: Proceedings of the 20th International Offshore (Ocean) and Polar Engineering Conference. CD-ROM.

Doong, D.J., Chuang, L.Z.H., Wu, L.C., Fan, Y.M., Kao, C.C., Wang, J.H., 2012. Development of an operational coastal flooding early warning system. Nat. Hazards Earth Syst. Sci. 12(2), 379−390. http://dx.doi.org/10.5194/nhess-12-379-2012.

Fan, Y.M., Pan, S.Q., Chen, J.M., Kao, C.C., 2013. Ensemble wave forecasting over typhoon period. OCEANS13 MTS/IEEE, pp. 1−7. http://dx.doi.org/10.1109/OCEANS-Bergen.2013.6608029.

Hunt, K.J., Irwin, G., Warwick, K., 1995. Neural Network Engineering in Dynamic Control Systems: Advances in Industrial Control. Springer, Berlin, p. 278.

Komen, G.J., Cavaleri, L., Donelan, M., Hasselmann, K., Hasselmann, S., Janssen, P.E.A.M., 1994. Dynamics and Modelling of Ocean Waves. Cambridge University Press, Cambridge, p. 532.

Lin, Y.P., Fan, Y.M., Wu, L.C., 2015. Innovative technologies for safer coasts in observation and forecasting. J. Ocean Underw. Technol. 25(2), 37−45 (in Chinese).

Liu, P.C., Chen, H.S., Doong, D.J., Kao, C.C., Hsu, Y.J.G., 2008. Monstrous ocean waves during typhoon Krosa. Ann. Geophys. 26(6), 1327−1329. http://dx.doi.org/10.5194/angeo-26-1327-2008.

Osuna, P., Wolf, J., Ashworth, M., 2004. Implementation of a Wave-current Interaction Module for the POLCOMS System, Internal Document No. 168. Proudman Oceanographic Laboratory, Liverpool.

Tolman, H.L., 1997. User Manual and System Documentation of WAVEWATCH-III Version 1.15, Technical Note 151. NOAA/NWS/NCEP/OMB, Camp Springs, p. 97.

Tolman, H.L., 1999. User Manual and System Documentation of WAVEWATCH-III Version 1.18, Technical Note 166. NOAA/NWS/NCEP/OMB, Camp Springs, p. 110.

Tolman, H.L., 2009. User Manual and System Documentation of WAVEWATCH III Version 3.14, Technical Note 276. NOAA/NWS/NCEP/OMB, Camp Springs, p. 194, Appendices.

The Wave Model Development and Implementation Group (WAMDIG), 1988. The WAM model: A third generation ocean wave prediction model. J. Phys. Oceanogr. 18(12), 1775−1810. http://dx.doi.org/10.1175/1520-0485(1988)018<1775:TWMTGO>2.0.CO;2.

Zou, Q.P., Chen, Y.P., Cluckie, I., Hewston, R., Pan, S.Q., Peng, Z., Reeve, D., 2013. Ensemble prediction of coastal flood risk arising from overtopping by linking meteorological, ocean, coastal and surf zone models. Q. J. R. Meteorol. Soc. 139(671), 298−313. http://dx.doi.org/10.1002/qj.2078.